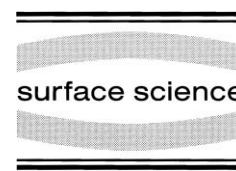




ELSEVIER

Surface Science 449 (2000) 125–134



www.elsevier.nl/locate/susc

# Surface-state electrical conduction on the Si(111)- $\sqrt{3} \times \sqrt{3}$ -Ag surface with noble-metal adatoms

Xiao Tong<sup>a,\*</sup>, Chun Sheng Jiang<sup>a</sup>, Kotaro Horikoshi<sup>a</sup>, Shuji Hasegawa<sup>a,b</sup>

<sup>a</sup> Department of Physics, School of Science, University of Tokyo, Hongo 7-3-1, Bunkyo-ku, Tokyo 113, Japan

<sup>b</sup> Core Research for Evolutional Science and Technology, The Japan Science and Technology Corporation, Kawaguchi Center Building, Hon-cho 4-1-8, Kawaguchi, Saitama 332-0012, Japan

Received 27 July 1999; accepted for publication 15 December 1999

## Abstract

The Si(111)- $\sqrt{21} \times \sqrt{21}$ -(Ag + Cu) superstructure was found to be induced by adsorption of about 0.14 monolayers (ML) of copper atoms on the Si(111)- $\sqrt{3} \times \sqrt{3}$ -Ag surface at room temperature (RT), which was quite similar to the cases of the  $\sqrt{21} \times \sqrt{21}$  superstructures induced by gold adsorption at RT and by silver adsorption at low temperature on the  $\sqrt{3} \times \sqrt{3}$ -Ag surface. Photoemission spectroscopies showed that the high electrical conductance observed for this copper-induced superstructure was due to a two-dimensional intrinsic dispersive surface-state band crossing the Fermi level, not due to the surface space-charge layer, which is again similar to the gold-induced  $\sqrt{21} \times \sqrt{21}$  surface. Each noble-metal adatom (gold, silver, copper) of less than ca. 0.1 ML coverage on the  $\sqrt{3} \times \sqrt{3}$ -Ag surface was found to exist commonly as two-dimensional adatom gas (2DAG) phase before they turned into the  $\sqrt{21} \times \sqrt{21}$  structure. The enhancement in surface conductance by the 2DAG phase was concluded to result from the donation of the adatoms' valence electrons into the surface-state band of the  $\sqrt{3} \times \sqrt{3}$ -Ag substrate. The difference in stability of the  $\sqrt{21} \times \sqrt{21}$  superstructures among gold-, silver- and copper-induced ones is discussed in terms of the first atomic ionization energy of the adatoms. © 2000 Elsevier Science B.V. All rights reserved.

**Keywords:** Copper; Electrical transport measurements; Photoelectron spectroscopy; Reflection high-energy electron diffraction (RHEED); Silicon; Silver; Surface electrical transport (surface conductivity, surface recombination, etc.); Surface electronic phenomena (work function, surface potential, surface states, etc.)

## 1. Introduction

In previous papers [1,2] we reported very high electrical conductances for the  $\sqrt{21} \times \sqrt{21}$  structures induced by gold or silver adsorption on the Si(111)- $\sqrt{3} \times \sqrt{3}$ -Ag surface at room or low tem-

perature, respectively. For the  $\sqrt{21} \times \sqrt{21}$ -(Ag + Au) surface, according to the results of photoemission spectroscopy, we confirmed that the high surface electrical conductances were not due to the surface-space charge layer but rather due to the formation of new dispersive surface-state bands crossing the Fermi level,  $E_F$  [3,4]. However, some questions still remaining drive us to investigate the  $\sqrt{21} \times \sqrt{21}$  surface further.

First, the mechanism of electrical conductance has been clarified for the  $\sqrt{21} \times \sqrt{21}$ -(Ag + Au) structure [1,3,4] but not yet clarified for the

\* Corresponding author. Fax: +81-48-462-4639.

E-mail address: tong@postman.riken.go.jp (X. Tong)

<sup>1</sup> Present address: Semiconductors Laboratory, The Institute of Physical and Chemical Research (RIKEN), Wako, Saitama 351-01, Japan.

$\sqrt{21} \times \sqrt{21}$ -(Ag+Ag) structure at low temperatures [2,5] because of less information about its electronic structure. The  $\sqrt{21} \times \sqrt{21}$  structure is known to be formed also by adsorption of copper on the  $\sqrt{3} \times \sqrt{3}$ -Ag surface at 753 K [7]; however, there are no reports about its atomic/electronic structures and electrical conductivity. Therefore, it is necessary to obtain more information for a systematic understanding of the  $\sqrt{21} \times \sqrt{21}$  superstructures induced by noble-metal adatoms on the  $\sqrt{3} \times \sqrt{3}$ -Ag surface.

Second, the stability of the  $\sqrt{21} \times \sqrt{21}$ -(Ag+Ag) structure depends sensitively on the substrate temperature [2]. When silver atoms are deposited on the  $\sqrt{3} \times \sqrt{3}$ -Ag surface at room temperature (RT), silver adatoms cannot form the  $\sqrt{21} \times \sqrt{21}$  superstructure but exist as a supersaturated two-dimensional adatom gas (2DAG) phase at coverages of less than 0.03 monolayers (ML) [8]. They begin to nucleate into three-dimensional (3D) silver microcrystals when the silver coverage exceeds 0.03 ML [8,9]. The 2DAG silver phase also shows a high surface conductance due to adatoms donating their valence electrons to the surface-state band of the  $\sqrt{3} \times \sqrt{3}$ -Ag substrate [9]. However, only below 250 K, the silver adatoms make the  $\sqrt{21} \times \sqrt{21}$  superstructure around 0.15 ML coverage [2]. Then, what is the relationship between the  $\sqrt{21} \times \sqrt{21}$  structure and the 2DAG phase?

Third, since the  $\sqrt{3} \times \sqrt{3}$ -Ag surface is known to have no dangling bonds, it is interesting to ask how the noble-metal adatoms make bonds with the substrate. In our previous papers, we proposed the simple concept of an atomic bonding mechanism in the  $\sqrt{21} \times \sqrt{21}$ -(Ag+Au) structure, referred to as ‘parasitic surface bonding’, in which the gold adatom shares its valence electron with an empty surface state of the substrate [4]. But, as shown in this paper, the  $\sqrt{21} \times \sqrt{21}$ -(Ag+Cu) structure is unstable compared with the  $\sqrt{21} \times \sqrt{21}$ -(Ag+Au) structure. The answer to this should be important for further understanding about ‘parasitic surface bonding’.

In this work, we studied the relationship among the changes in surface atomic/electronic structure and surface electrical conduction during adsorp-

tion of copper atoms on the Si(111)- $\sqrt{3} \times \sqrt{3}$ -Ag surface at RT with reflection high-energy electron diffraction (RHEED), angle-resolved ultraviolet/X-ray photoelectron spectroscopies (ARUPS and XPS) and surface conductance measurements. Furthermore, by combining the present work with previous results for the silver- and gold-covered  $\sqrt{3} \times \sqrt{3}$ -Ag surfaces [2–4,9], the mechanism of surface conductance on the noble-metal adatom-covered  $\sqrt{3} \times \sqrt{3}$ -Ag surfaces and the stability of  $\sqrt{21} \times \sqrt{21}$  structures are systematically discussed.

## 2. Experiments

The experiments were carried out in an ultra-high vacuum (UHV) chamber whose base pressure was below  $5 \times 10^{-10}$  Torr. It consisted of a RHEED system, an X-ray source (non-monochromated Mg K $\alpha$  line), an ultraviolet (UV) light source (He I), an electron analyzer (VG ADES 500) [4], and a sample holder for four-probe electrical conductivity measurements [6]. The substrate was a p-type Si(111) wafer with 20  $\Omega$  cm resistivity at RT and its typical dimensions were 25 mm  $\times$  4 mm  $\times$  0.4 mm. A clear Si(111)- $7 \times 7$  RHEED pattern was produced by flashing the sample at 1500 K several times by passing a direct current (DC) of around 10 A through it. The  $\sqrt{3} \times \sqrt{3}$ -Ag surface was prepared by depositing 1 ML of silver at a constant rate of 0.66 ML min $^{-1}$  on the  $7 \times 7$  substrate maintained at 650 K. After cooling the substrate to RT, the  $\sqrt{21} \times \sqrt{21}$ -(Ag+Cu) superstructures were formed by depositing copper of about 0.14 ML coverage on the  $\sqrt{3} \times \sqrt{3}$ -Ag surface at a rate of 0.4 ML min $^{-1}$ . The amount of each metal deposited was monitored by a quartz oscillator.

## 3. Results

Fig. 1a shows the RHEED pattern of the  $\sqrt{21} \times \sqrt{21}$ -(Ag+Cu) structure induced by deposition of 0.14 ML of copper adatoms on the  $\sqrt{3} \times \sqrt{3}$ -Ag surface at RT. Weak and streaky diffraction spots in this RHEED pattern come

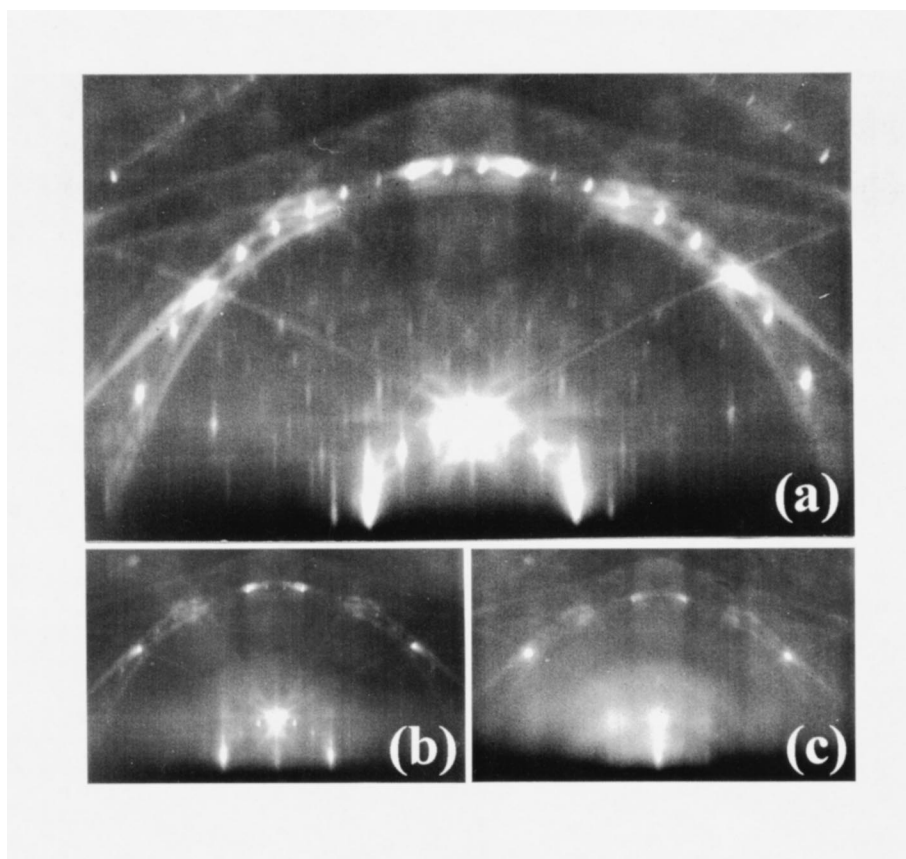


Fig. 1. RHEED patterns taken during copper adsorption on the Si(111)- $\sqrt{3} \times \sqrt{3}$ -Ag surface at RT with the electron beam in  $[11\bar{2}]$  incidence: (a) Si(111)- $\sqrt{21} \times \sqrt{21}$ -(Ag+Cu) structure induced by adsorption of about 0.14 ML of copper; (b)  $\sqrt{3} \times \sqrt{3}$ -(Ag+Cu) surface after 0.2 ML of copper deposition; (c) after deposition of 1.0 ML.

from two equivalent domains of the  $\sqrt{21} \times \sqrt{21}$  structure with  $\pm 10.89^\circ$  rotations with respect to the  $1 \times 1$  fundamental lattice of the Si(111) surface. With copper deposition beyond about 0.15 ML coverage, the  $\sqrt{21} \times \sqrt{21}$ -(Ag+Cu) structure disappeared rapidly and transformed into another  $\sqrt{3} \times \sqrt{3}$  structure (Fig. 1b). The intensity distribution of fractional-order spots in this  $\sqrt{3} \times \sqrt{3}$ -(Ag+Cu) pattern was different from that in the initial  $\sqrt{3} \times \sqrt{3}$ -Ag pattern; the  $(1/3, 1/3)$  spots were stronger than  $(2/3, 2/3)$  spots, while the initial  $\sqrt{3} \times \sqrt{3}$ -Ag pattern had the opposite relative intensity. Streaks and halos emerged with further copper deposition as shown in Fig. 1c.

Fig. 2 shows the change in electrical conductance of the silicon wafer during this copper deposi-

tion on the Si(111)- $\sqrt{3} \times \sqrt{3}$ -Ag surface at RT. The structural changes shown in Fig. 1 are also indicated in this figure. When the evaporator shutter was opened, with the appearance of the  $\sqrt{21} \times \sqrt{21}$  spots and gaining the maximum intensity at about 0.14 ML coverage, the conductance increased steeply by  $1.7 \times 10^{-4} \text{ S } \square^{-1}$  from that of the initial  $\sqrt{3} \times \sqrt{3}$ -Ag surface. Then, with the disappearance of the  $\sqrt{21} \times \sqrt{21}$  superstructure with further copper deposition, the conductance dropped back. From about 0.5 ML coverage, streaks and halos emerged (see Fig. 1c), and the conductance began to increase slowly again until the deposition was stopped. The above behavior in conductance change means that the  $\sqrt{21} \times \sqrt{21}$ -(Ag+Cu) surface has a higher surface

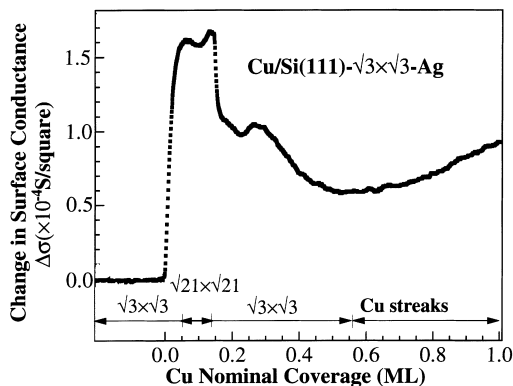


Fig. 2. Conductance changes of the silicon wafer during copper adsorption on the Si(111)- $\sqrt{3}\times\sqrt{3}$ -Ag surface at RT. The surface structure changes are also indicated in the corresponding coverage ranges.

electrical conductance than the initial  $\sqrt{3}\times\sqrt{3}$ -Ag surface, which is similar to the case of the Si(111)- $\sqrt{21}\times\sqrt{21}$ -(Ag+Au) [1,3] and Si(111)- $\sqrt{21}\times\sqrt{21}$ -(Ag+Ag) structures [2].

Figs. 3a and b show ARUPS spectra taken from the initial  $\sqrt{3}\times\sqrt{3}$ -Ag and the  $\sqrt{21}\times\sqrt{21}$ -(Ag+Cu) surfaces, respectively. The excitation light was illuminated in a direction of  $30^\circ$  from the surface normal. The electron emission angles  $\theta_e$  were changed from the surface normal to the  $[10\bar{1}]$  direction. For the initial  $\sqrt{3}\times\sqrt{3}$ -Ag surface (Fig. 3a), a dispersive peak with weak intensity near  $E_F$ , indicated by small arrowheads, can be observed at emission angles of  $32^\circ$  and  $33^\circ$ . This was called the  $S_1$  surface-state band [4,10,11], making a small electron pocket having a parabolic dispersion around the  $\bar{\Gamma}$  point in the  $\sqrt{3}\times\sqrt{3}$  surface Brillouin zone (SBZ), as shown in Fig. 4a (open circles), while for the  $\sqrt{21}\times\sqrt{21}$ -(Ag+Cu) surface (Fig. 3b) two series of dispersive peaks appear near  $E_F$  as indicated by big and small arrowheads; here we call them  $S_1^*$  and  $S_1'$  bands, respectively. The  $S_1'$  band seems to be similar to the  $S_1$  band of the initial  $\sqrt{3}\times\sqrt{3}$ -Ag structure, but the  $S_1^*$  band is not observed on the initial  $\sqrt{3}\times\sqrt{3}$ -Ag surface.

Fig. 4b shows the two-dimensional band-dispersion diagram near  $E_F$  for the  $\sqrt{21}\times\sqrt{21}$ -(Ag+Cu) surface (open circles) obtained from Fig. 3b. For comparison, Fig. 4 also shows the

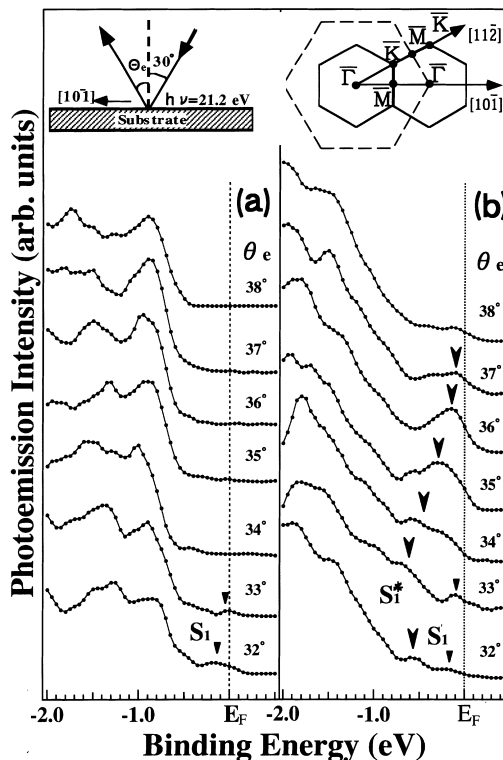


Fig. 3. ARUPS spectra taken from (a) the Si(111)- $\sqrt{3}\times\sqrt{3}$ -Ag surface and (b) the Si(111)- $\sqrt{21}\times\sqrt{21}$ -(Ag+Cu) surface. The excitation light was He I (21.2 eV) and its incidence angle was  $30^\circ$  from the surface-normal direction. The electron emission angles were changed towards the  $[10\bar{1}]$  direction.

bands for the initial Si(111)- $\sqrt{3}\times\sqrt{3}$ -Ag surface (open circles in a), the  $\sqrt{3}\times\sqrt{3}$ -Ag surface covered by 0.1 ML of gold (closed circles in a) and the gold-induced  $\sqrt{21}\times\sqrt{21}$  surface (crosses and solid circles in b) [4]. It is found that the dispersions of the  $S_1^*$  and  $S_1'$  bands of the  $\sqrt{21}\times\sqrt{21}$ -(Ag+Cu) structure are extremely similar to those of the  $\sqrt{21}\times\sqrt{21}$ -(Ag+Au) structure. Both the  $S_1^*$  and  $S_1'$  bands appear around the  $\bar{\Gamma}$  point of the  $\sqrt{3}\times\sqrt{3}$  SBZ, which is similar to the  $S_1$  band of the initial  $\sqrt{3}\times\sqrt{3}$ -Ag structure. However, the bottom of the  $S_1^*$  band is much lower below  $E_F$  than that of the  $S_1'$  and  $S_1$  bands.

We also measured Si 2p core-level emissions in XPS under bulk-sensitive conditions at RT, from the clean Si(111)- $7\times 7$ , the initial  $\sqrt{3}\times\sqrt{3}$ -Ag and the  $\sqrt{21}\times\sqrt{21}$ -(Ag+Cu) surfaces. Compared with those on the clean Si(111)- $7\times 7$  surface, the peaks

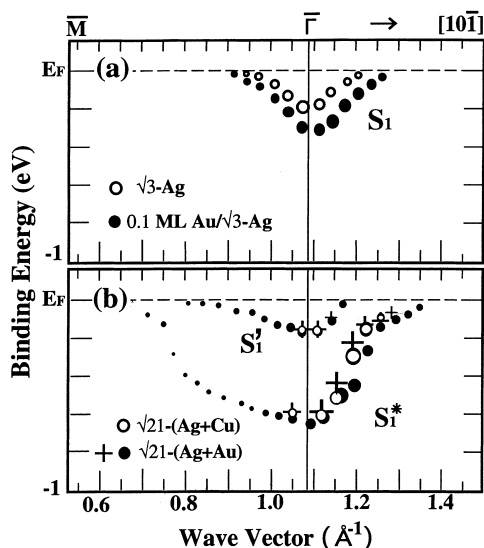


Fig. 4. Two-dimensional band-dispersion diagram near the Fermi level for the  $\sqrt{3} \times \sqrt{3}$ -Ag surface with noble-metal adatoms. (a) Open circles are for the initial Si(111)- $\sqrt{3} \times \sqrt{3}$ -Ag surface, and closed circles for the  $\sqrt{3} \times \sqrt{3}$ -Ag surface covered by 0.1 ML of gold [4]. (b) Open circles represent the  $S_1^*$  and  $S_1'$  peak positions in Fig. 3b obtained from the  $\sqrt{21} \times \sqrt{21}$ -(Ag+Cu) structure. The crosses and solid circles show the states obtained from the gold-induced  $\sqrt{21} \times \sqrt{21}$  surface with  $30^\circ$  and  $0^\circ$  incidence of UV light, which were obtained in this experiment (ARUPS spectra are not shown here) and in our previous paper [4], respectively. Their sizes correspond qualitatively to the intensity of the respective peaks. The symbols  $\bar{\Gamma}$  and  $\bar{M}$  are symmetric points in a  $\sqrt{3} \times \sqrt{3}$  surface Brillouin zone.

of the Si 2p core-level emission shift towards  $E_F$  by about 0.47 eV and 0.30 eV for the  $\sqrt{3} \times \sqrt{3}$ -Ag and  $\sqrt{21} \times \sqrt{21}$ -(Ag+Cu) surface, respectively. Since  $E_F$  at the clean  $7 \times 7$  surface is known to be located at 0.63 eV above the valence-band maximum [12,13], it is easily obtained that  $E_F$  positions are at 0.16 eV and 0.33 eV above the valence-band maximum for the  $\sqrt{3} \times \sqrt{3}$ -Ag and  $\sqrt{21} \times \sqrt{21}$ -(Ag+Cu) surface, respectively. The detailed dependence of the position of  $E_F$  on copper coverage on the  $\sqrt{3} \times \sqrt{3}$ -Ag surface is shown by open circles in Fig. 5, which shows quite a similarity between copper and gold adsorptions. For the silicon wafer of p-type used in this experiment, the distance between  $E_F$  and the valence-band maximum in the bulk is 0.29 eV, estimated from the resistivity [14]. Therefore, the band bend-

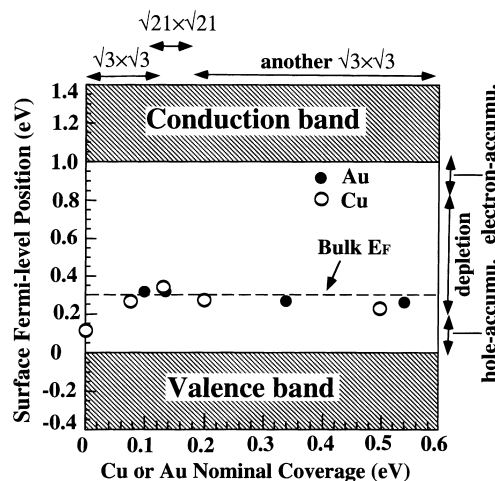


Fig. 5. The shifts of the surface Fermi-level position as a function of copper (gold) coverage. These were determined from the peak shift of Si 2p core-level emission in XPS during copper (gold) deposition on the Si(111)- $\sqrt{3} \times \sqrt{3}$ -Ag surface at room temperature.

ings in the surface space-charge layer for the  $\sqrt{3} \times \sqrt{3}$ -Ag and  $\sqrt{21} \times \sqrt{21}$ -(Ag+Cu) surfaces are obtained as shown in Fig. 6. The surface states observed at the  $\sqrt{3} \times \sqrt{3}$ -Ag and  $\sqrt{21} \times \sqrt{21}$ -(Ag+Cu) surfaces are also shown schematically in Fig. 6 [4]. It clearly indicates that, during conversion from the  $\sqrt{3} \times \sqrt{3}$ -Ag structure to the  $\sqrt{21} \times \sqrt{21}$ -(Ag+Cu) one, the excess holes accumulated in the surface space-charge layer are completely depleted, accompanied by the  $S_1$  surface-state band transforming into the  $S_1^*$  and  $S_1'$  bands.

Fig. 7 shows the resistance changes of a silicon wafer during intermittent depositions of noble-metal atoms on the Si(111)- $\sqrt{3} \times \sqrt{3}$ -Ag surface at various temperatures. Upon beginning the deposition the resistance decreases steeply for all cases, and then, by interrupting the deposition below 0.1 ML coverage, the resistances are kept constant, independent of the temperature and adatom species, while RHEED indicates that the surface still remains in the  $\sqrt{3} \times \sqrt{3}$  structure and the  $\sqrt{21} \times \sqrt{21}$  diffraction spots do not appear yet. With starting the deposition again the resistances begin to decrease further, accompanied with the structure conversion into the  $\sqrt{21} \times \sqrt{21}$  surface for all cases. After passing through the minimum

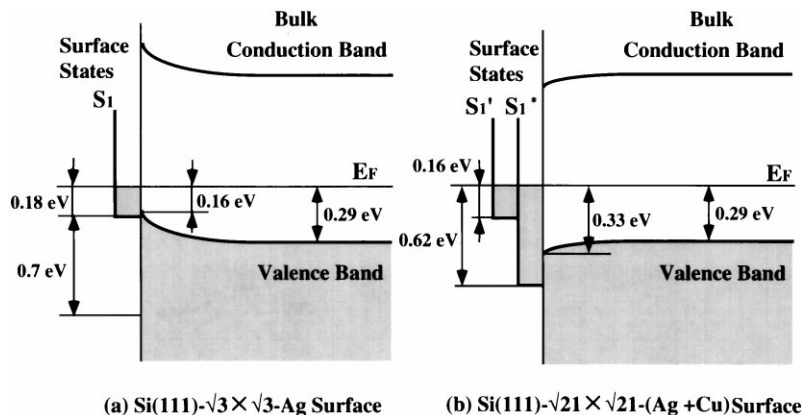


Fig. 6. Schematic illustration of the surface states and band bending at (a) the Si(111)- $\sqrt{3}\times\sqrt{3}$ -Ag surface and (b) the Si(111)- $\sqrt{21}\times\sqrt{21}$ -(Ag+Cu) surface. They are obtained from the results of ARUPS and XPS. (b) is also applicable for the  $\sqrt{21}\times\sqrt{21}$ -(Ag+Au) structure [4].

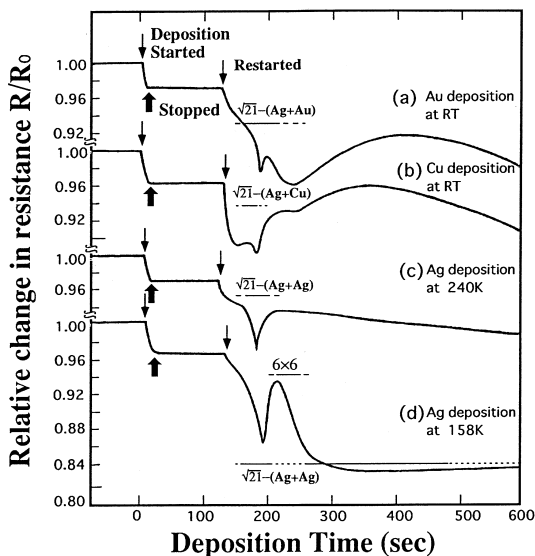


Fig. 7. The resistance changes of a silicon wafer during intermittent depositions of noble-metal adatoms on the  $\sqrt{3}\times\sqrt{3}$ -Ag surface at various temperatures. Downward arrows indicate the starting points of depositions, and upward arrows their end points. The coverage at the end points is less than 0.1 ML. The surface structure changes are also indicated, along with the resistance changes. The  $\sqrt{3}\times\sqrt{3}$  fractional spots were always observed throughout these observations.

resistances, the resistances turn to increase with further depositions, accompanied with another  $\sqrt{3}\times\sqrt{3}$  phase or  $6\times 6$  structure appearing,

depending on the temperature and noble-metal species.

#### 4. Discussion

For the silver-induced low-temperature and gold-induced RT  $\sqrt{21}\times\sqrt{21}$  structures, scanning tunneling microscopy (STM) images [5] and RHEED rocking curves [15] indicate extremely similar atomic arrangements. Here, Fig. 4b indicates that the  $\sqrt{21}\times\sqrt{21}$ -(Ag+Cu) electronic structure at the vicinity of  $E_F$  is quite similar to that of the gold-induced  $\sqrt{21}\times\sqrt{21}$  structure [4]. Additionally, the three kinds of  $\sqrt{21}\times\sqrt{21}$  structure commonly have high surface conductances compared with the initial  $\sqrt{3}\times\sqrt{3}$ -Ag surface [1,2]. This suggests that these three  $\sqrt{21}\times\sqrt{21}$  structures induced by adsorptions of noble-metal atoms on the  $\sqrt{3}\times\sqrt{3}$ -Ag surface possibly have the same atomic arrangement and electronic structure. Recent first-principles calculations about the  $\sqrt{3}\times\sqrt{3}$ -Ag surface with periodically adsorbed silver adatoms reproduce an electronic band structure near  $E_F$  similar to our experimental results in Fig. 4b [16], which may be a feature common to all of the noble-metal adatoms on the  $\sqrt{3}\times\sqrt{3}$ -Ag surface.

However, the RHEED diffraction spots in the

$\sqrt{21} \times \sqrt{21}$ -(Ag+Cu) structure are weaker and broader than those of the gold-induced  $\sqrt{21} \times \sqrt{21}$  phase; this means that the total area fraction and average size of the  $\sqrt{21} \times \sqrt{21}$ -(Ag+Cu) domains on the  $\sqrt{3} \times \sqrt{3}$ -Ag surface are smaller than those of the  $\sqrt{21} \times \sqrt{21}$ -(Ag+Au) surface. For the saturated  $\sqrt{21} \times \sqrt{21}$ -(Ag+Au) surface, STM observations indicate that about 85% of the  $\sqrt{3} \times \sqrt{3}$ -Ag surface is covered by the  $\sqrt{21} \times \sqrt{21}$ -(Ag+Au) domains [17]. Thus it can be concluded that the surface probed by RHEED in Fig. 1 must be a mixture of  $\sqrt{21} \times \sqrt{21}$ -(Ag+Cu) and  $\sqrt{3} \times \sqrt{3}$ -Ag phases, which is consistent with our recent STM observations. Additionally, the RHEED spots in the  $\sqrt{21} \times \sqrt{21}$ -(Ag+Cu) phases gradually disappeared after a lapse of about 5 h just by leaving the sample in UHV, leaving only the  $\sqrt{3} \times \sqrt{3}$  spots, while they are stable in the  $\sqrt{21} \times \sqrt{21}$ -(Ag+Au) phases. This means that the  $\sqrt{21} \times \sqrt{21}$ -(Ag+Cu) structure is less stable than the  $\sqrt{21} \times \sqrt{21}$ -(Ag+Au).

As shown in Figs. 3 and 4, two dispersive bands  $S_1$  and  $S_1^*$  near the  $E_F$  level are observed in the  $\sqrt{21} \times \sqrt{21}$ -(Ag+Au) and  $\sqrt{21} \times \sqrt{21}$ -(Ag+Cu) surfaces. Because the  $S_1$  band at the  $\sqrt{21} \times \sqrt{21}$  surface is very similar to the  $S_1$  band at the initial clean  $\sqrt{3} \times \sqrt{3}$ -Ag surface, we suggest that the  $S_1$  band is partly contributed from the remaining  $\sqrt{3} \times \sqrt{3}$ -Ag domains on the surfaces. This suggestion is supported by our recent results that only the  $S_1^*$  band is observed without the  $S_1$  band from the  $\sqrt{21} \times \sqrt{21}$ -(Ag+Ag) surface in which there is no  $\sqrt{3} \times \sqrt{3}$ -Ag domains remaining, as found by ARUPS measurements at low temperature [18]. The  $S_1^*$  band in the  $\sqrt{21} \times \sqrt{21}$  phase appears only around the  $\bar{\Gamma}$  point of the  $\sqrt{3} \times \sqrt{3}$  SBZ, which is similar to the  $S_1$  band of the initial  $\sqrt{3} \times \sqrt{3}$ -Ag structure, and its intensity is stronger and its bottom much lower below  $E_F$  than that of the  $S_1$  band of the initial  $\sqrt{3} \times \sqrt{3}$ -Ag phase. These facts imply that the  $S_1^*$  band seems to be modulated from the  $S_1$  band by accumulating more electrons into the  $S_1$  band of the initial  $\sqrt{3} \times \sqrt{3}$ -Ag [4]. Because the holes accumulated in the surface space-charge layer below the initial  $\sqrt{3} \times \sqrt{3}$ -Ag are depleted as shown in Fig. 6, the electrons in

the  $S_1^*$  band are not from the substrate bulk, but should be from the copper (gold) adatoms [4].

For copper- and gold-induced  $\sqrt{21} \times \sqrt{21}$  surfaces, the dispersion and intensity of the  $S_1^*$  band are quite similar to each other as indicated in Fig. 4b, meaning that similar numbers of surface-state electrons are trapped in these bands on both surfaces. Because the total area fraction covered by the  $\sqrt{21} \times \sqrt{21}$ -(Ag+Cu) domains on the  $\sqrt{3} \times \sqrt{3}$ -Ag surface is less than that of the  $\sqrt{21} \times \sqrt{21}$ -(Ag+Au) surface, the amount of charge transferred from each copper adatom into the bands must be larger than that of gold adatoms in the  $\sqrt{21} \times \sqrt{21}$ -(Ag+Au) phase. This means that the degree of ionization of copper adatoms is larger than that of gold, which is consistent with the difference in the first atomic ionization energy: 8.0 eV (copper) and 9.3 eV (gold). Then the repulsive reaction among the adatoms would be stronger for copper than gold adatoms in the  $\sqrt{21} \times \sqrt{21}$  structures. Thus the reasons why the  $\sqrt{21} \times \sqrt{21}$ -(Ag+Cu) structure is less stable than the  $\sqrt{21} \times \sqrt{21}$ -(Ag+Au) structure may be partly interpreted qualitatively by the difference in the first atomic ionization energy of the adatoms.

Next, we discuss the mechanism of surface electrical conductance of the  $\sqrt{21} \times \sqrt{21}$ -(Ag+Cu) surface. Electrical conduction near the semiconductor surface is generally classified into three types, each of which is in principle closely related to the surface structures [19]: conduction through the grown metal atomic layers, through the surface space-charge layer of the substrate, and through the surface-state bands.

The 0.14 ML of copper coverage necessary for forming the  $\sqrt{21} \times \sqrt{21}$ -(Ag+Cu) structure is too small to make percolation paths on 2D triangular lattices. And the electrical conduction through the surface space-charge layer should be suppressed at the  $\sqrt{21} \times \sqrt{21}$ -(Ag+Cu) surface because the excess holes accumulated in the surface space-charge layer below the initial  $\sqrt{3} \times \sqrt{3}$ -Ag surface are depleted by copper adsorption as indicated in Fig. 6. Therefore, the conductance increase with formation of the  $\sqrt{21} \times \sqrt{21}$  structure measured in Fig. 2 cannot be explained by the conduction through the grown metal atomic layers nor the

surface space-charge layer. On the other hand, the  $S_1^*$  band does not exist on the initial  $\sqrt{3} \times \sqrt{3}$ -Ag surface, but only on the  $\sqrt{21} \times \sqrt{21}$  surfaces, and it is occupied by more electrons than the  $S_1$  band of the initial  $\sqrt{3} \times \sqrt{3}$ -Ag phase as shown in Fig. 4. Thus we can conclude that the observed excess conductance on the  $\sqrt{21} \times \sqrt{21}$  structure is due to the newly formed surface state  $S_1^*$ . For the  $\sqrt{3} \times \sqrt{3}$ -(Ag+Cu) surface prepared by further copper deposition on the  $\sqrt{21} \times \sqrt{21}$ -(Ag+Cu) structure, the decrease in conductance can be attributed to the disappearance of the  $\sqrt{21} \times \sqrt{21}$  structure and the  $S_1^*$  band.

Finally, we discuss the relationship between the electrical conduction of the 2DAG and  $\sqrt{21} \times \sqrt{21}$  phases. RHEED indicates that less than 0.1 ML of noble-metal adatoms is not enough for structural conversion from the  $\sqrt{3} \times \sqrt{3}$  into the  $\sqrt{21} \times \sqrt{21}$  structures. For the 0.1 ML gold-covered  $\sqrt{3} \times \sqrt{3}$ -Ag surface, photoelectron spectroscopies indicate that more electrons occupy the  $S_1$  band compared with the case for the initial  $\sqrt{3} \times \sqrt{3}$ -Ag surface as shown in Fig. 4a (closed circles) [4]. Because the excess holes accumulated in the surface space-charge layer below the initial  $\sqrt{3} \times \sqrt{3}$ -Ag surface are depleted for the 0.1 ML gold-covered  $\sqrt{3} \times \sqrt{3}$ -Ag surface as indicated in Fig. 5, the extra electrons in the  $S_1$  band are donated by the gold adatoms, and the surface space-charge layer plays no roles in the conductance increase. This means that the enhancement in surface conductance by adsorption of 0.1 ML of gold on the  $\sqrt{3} \times \sqrt{3}$ -Ag surface, as shown in Fig. 7a, originates from the gold adatoms donating electrons into the surface-state band  $S_1$  of the  $\sqrt{3} \times \sqrt{3}$ -Ag substrate. Similar changes of surface conductance and the  $S_1$  band were also observed from the additional 0.03 ML of silver adsorption on the  $\sqrt{3} \times \sqrt{3}$ -Ag surface at RT, in which the silver adatoms exist on the surface as a supersaturated metastable two-dimensional adatom gas (2DAG) phase [9]. The ‘frozen’ 2DAG on the  $\sqrt{3} \times \sqrt{3}$ -Ag surface is observed by STM only at low temperature [5], while at RT the adatoms migrate on the surface so fast that STM cannot catch them. As shown in Fig. 7c and d, the ‘frozen’ 2DAG also results in an enhancement of surface

conductance before it turns into the  $\sqrt{21} \times \sqrt{21}$  structure. This indicates that, irrespective of the 2DAG being moving or frozen, they can donate electrons into the  $S_1$  band, resulting in a similar enhancement of surface conductance. According to the above discussion we can conclude that, before formation of the  $\sqrt{21} \times \sqrt{21}$  structure, noble-metal adatoms with smaller coverages exist commonly as 2DAG on the  $\sqrt{3} \times \sqrt{3}$ -Ag surface. The enhancement of surface conductance by the 2DAG phase is due to electron donation by the adatoms into the surface-state band  $S_1$  of the initial  $\sqrt{3} \times \sqrt{3}$ -Ag substrate.

According to Fig. 7a, the  $\sqrt{21} \times \sqrt{21}$ -(Ag+Au) and gold-induced 2DAG phases have higher surface-state conductance than the  $\sqrt{3} \times \sqrt{3}$ -Ag phase by  $(2.0 \pm 0.3) \times 10^{-4} \text{ S } \square^{-1}$  and  $(0.7 \pm 0.1) \times 10^{-4} \text{ S } \square^{-1}$ , respectively. The  $\sqrt{3} \times \sqrt{3}$ -Ag surface has a higher surface-state conductance than the clean  $7 \times 7$  surface by  $(0.8 \pm 0.1) \times 10^{-4} \text{ S } \square^{-1}$  [3]. Since, on the other hand, the conductance through a surface state on the  $7 \times 7$  surface is actually estimated to be of the order of  $10^{-9} \text{ S } \square^{-1}$  from STM images [20], the total conductances via the surface state on the  $\sqrt{21} \times \sqrt{21}$ -(Ag+Au) and 2DAG gold surfaces are  $\sigma_{\sqrt{21}} = (2.8 \pm 0.4) \times 10^{-4} \text{ S } \square^{-1}$  and  $\sigma_{2\text{DAG}} = (1.5 \pm 0.2) \times 10^{-4} \text{ S } \square^{-1}$ , respectively. If both the  $S_1$  and  $S_1^*$  bands are assumed to be a 2D free-electron band, the mobility and the mean free path of 2D free electrons are given by  $\mu = 2\pi\sigma/k_F^2 e$  and  $l = (h\sigma)/(k_F e^2)$ , respectively, where  $\sigma$  is the sheet conductance,  $k_F$  is the Fermi wave number and  $e$  is the elementary charge. By using  $k_{F\sqrt{21}} = (0.32 \pm 0.03) \text{ \AA}^{-1}$  for the  $S_1^*$  band and  $k_{F2\text{DAG}} = (0.15 \pm 0.02) \text{ \AA}^{-1}$  for the  $S_1$  band, as indicated in Fig. 4, we can estimate  $\mu_{\sqrt{21}} = (12 \pm 4) \text{ cm}^2 \text{ V}^{-1} \text{ s}^{-1}$ ,  $\mu_{2\text{DAG}} = (26 \pm 6) \text{ cm}^2 \text{ V}^{-1} \text{ s}^{-1}$ ,  $l_{\sqrt{21}} = (24 \pm 6) \text{ \AA}$  and  $l_{2\text{DAG}} = (26 \pm 9) \text{ \AA}$ . STM observations indicate that both structures of the saturated frozen 2DAG and  $\sqrt{21} \times \sqrt{21}$  phases are formed by 2D nuclei consisting of a few adatoms [5]: the 2D nuclei arrange randomly in the saturated 2DAG phase, and the average distance among the center of 2D nuclei on terraces is about  $24 \pm 7 \text{ \AA}$ , while in the  $\sqrt{21} \times \sqrt{21}$  phase, the 2D nuclei arrange in an order with  $\sqrt{21}a_0 = 17 \text{ \AA}$

periodicity, where  $a_0$  is the length of the  $1 \times 1$  surface unit vector. Therefore, the estimated mean free path is roughly equal to the average separation among the 2D nuclei in both 2DAG and  $\sqrt{21} \times \sqrt{21}$  phases, suggesting that 2D nuclei in the both phases act as carrier-scattering centers. The gold adatoms in the 2DAG and  $\sqrt{21} \times \sqrt{21}$  phases not only donate electrons into the surface-state bands, but also scatter carriers.

The estimated electron mobilities of both phases are much smaller than the bulk parameter  $\mu_{\text{bulk}}$  of about  $1500 \text{ cm}^2 \text{ V}^{-1} \text{ s}^{-1}$  for conduction electrons at RT. This may be because of severe carrier scattering by gold adatoms in the 2DAG and  $\sqrt{21} \times \sqrt{21}$  phases, defects, domain boundaries and steps on the surfaces. On the other hand, as shown in Fig. 4, since in the vicinity of  $E_F$  the  $S_1$  band seems to disperse more steeply than the  $S_1^*$  band, the effective mass of the conduction electrons in the  $S_1^*$  band at the  $\sqrt{21} \times \sqrt{21}$  phases is larger than that of the  $S_1$  band on the 2DAG phases. This may be the reason why the estimated carrier mobility in the  $S_1^*$  band is smaller than that of the  $S_1$  band of the 2DAG phase. Therefore, the higher electrical conductance of the  $\sqrt{21} \times \sqrt{21}$  phase compared with that of the 2DAG phase, as shown in Fig. 7, has to be mainly attributed to the increase in the number of electrons in the  $S_1^*$  band of the  $\sqrt{21} \times \sqrt{21}$  phases compared with that in the  $S_1$  band of the 2DAG phase.

## 5. Summary

1. The Si(111)- $\sqrt{21} \times \sqrt{21}$ -(Ag+Cu) superstructure was found to be induced by adsorption of about 0.14 ML of copper atoms on the  $\sqrt{3} \times \sqrt{3}$ -Ag surface at RT, and to have a high surface electrical conductance compared with the initial  $\sqrt{3} \times \sqrt{3}$ -Ag surface. Photoemission spectroscopies showed that this  $\sqrt{21} \times \sqrt{21}$ -(Ag+Cu) structure had intrinsic dispersive surface-state bands,  $S_1^*$  and  $S_1'$ , crossing the Fermi level, while the surface space-charge layer in the substrate was a depletion layer. Then it was concluded that the observed excess surface con-

ductance was due to the two-dimensional bands of the surface electronic state. These behaviors in electronic structure and surface conductance are quite similar to the case of the  $\sqrt{21} \times \sqrt{21}$ -(Ag+Au) structure in our previous reports.

2. Noble-metal adatoms at small coverage (less than ca. 0.1 ML) on the  $\sqrt{3} \times \sqrt{3}$ -Ag surface were suggested to exist commonly as 2DAG phases before they turned into the  $\sqrt{21} \times \sqrt{21}$  superstructures. The enhancement in surface conductance by the 2DAG adsorption results from the adatoms donating their valence electrons into the surface-state band  $S_1$  of the  $\sqrt{3} \times \sqrt{3}$ -Ag substrate. The carrier mobility of the surface-state electrons was estimated to be larger for the 2DAG phase than for the  $\sqrt{21} \times \sqrt{21}$  phase. This means that the noble-metal adatoms in the 2DAG and  $\sqrt{21} \times \sqrt{21}$  phases not only donate electrons into the surface-state band to enhance the surface conductance, but also act as carrier-scattering centers.
3. The difference in stability of the  $\sqrt{21} \times \sqrt{21}$ -(Ag+Cu) and  $\sqrt{21} \times \sqrt{21}$ -(Ag+Au) structures at RT is suggested to be influenced by a difference in degree of ionization of the adatoms, which is governed by their first atomic ionization energy.

## Acknowledgements

We acknowledge Professor M. Henzler of Hannover University for his valuable discussions. This work was supported in part by Grants-In-Aid from the Ministry of Education, Science, Culture, and Sports of Japan, especially through the Grants-In-Aid for Creative Basic Research (No. 09NP120). We were supported also by CREST (Core Research for Evolutional Science and Technology) of the Japan Science and Technology Corporation (JST).

## References

- [1] C.-S. Jiang, X. Tong, S. Hasegawa, Surf. Sci. 376 (1997) 69.
- [2] X. Tong, S. Hasegawa, S. Ino, Phys. Rev. B 55 (1997) 1310.

- [3] S. Hasegawa, X. Tong, C.-S. Jiang, Y. Nakajima, T. Nagao, Surf. Sci. 386 (1997) 322.
- [4] X. Tong, C.S. Jiang, S. Hasegawa, Phys. Rev. B 57 (1998) 9015.
- [5] X. Tong, Y. Sugiura, T. Nagao, T. Takami, S. Takeda, S. Ino, S. Hasegawa, Surf. Sci. 408 (1998) 146.
- [6] S. Hasegawa, S. Ino, Phys. Rev. Lett. 68 (1992) 1192.
- [7] I. Homma, Y. Tanishiro, K. Yagi, in: S.Y. Tong, M.A. Van Hove, K. Takayanagi, X.D. Xie (Eds.), The Structure of Surface vol. III, Springer, Berlin, 1991, p. 610.
- [8] Y. Nakajima, G. Uchida, T. Nagao, S. Hasegawa, Phys. Rev. B 54 (1996) 14134.
- [9] Y. Nakajima, S. Takeda, T. Nagao, S. Hasegawa, X. Tong, Phys. Rev. B 56 (1997) 6782.
- [10] L.S.O. Johansson, E. Landemark, C.J. Karlsson, R.I.G. Uhrberg, Phys. Rev. Lett. 69 (1992) 2451.
- [11] H. Aizawa, M. Tsukada, N. Sato, S. Hasegawa, Surf. Sci. 429 (1999) L509.
- [12] F.J. Himpsel, G. Hollinger, R.A. Pollack, Phys. Rev. B 28 (1983) 7014.
- [13] J. Viernow, M. Henzler, W.L. O'Brien, F.K. Men, F.M. Leible, D.Y. Petrovyleh, J.L. Lin, F.J. Himpsel, Phys. Rev. B 57 (1998) 2321.
- [14] C.S. Jiang, S. Hasegawa, S. Ino, Phys. Rev. 54 (1996) 10389.
- [15] M. Lijadi, H. Iwashige, A. Ichimiya, Surf. Sci. 357/358 (1996) 51.
- [16] H. Aizawa, M. Tsukada, Phys. Rev. B 59 (1999) 10923.
- [17] J. Nogami, K.J. Wan, X.F. Lin, Surf. Sci. 306 (1994) 81.
- [18] X. Tong, S. Ohuchi, T. Tanikawa, T. Sekiguchi, K. Hori-kosi, I. Matuda, T. Nagao, Y. Aoyagi, S. Hasegawa, in preparation.
- [19] M. Henzler, in: J.M. Blakely (Ed.), Surface Physics of Materials vol. I, Academic Press, New York, 1975, p. 241.
- [20] S. Heike, S. Watanabe, Y. Wada, T. Hashizume, Phys. Rev. Lett. 81 (1998) 890.